Journal of Marine Research, 58, 375–403, 2000

Emergence of modons from collapsing vortex structures on the β-plane

by Z. Kizner[1] and D. Berson[1]

ABSTRACT

The evolution of unstable barotropic vortices is studied numerically. Exact solutions to the equation of potential vorticity conservation under the "rigid lid" condition, as well as nonsteady-state configurations, are set as initial states in the evolutionary experiments. The examined "shielded modon" structures usually collapse within one to several synoptic periods and radiate vortex pairs propagating westward and eastward. The latter are shown to be modons of Larichev and Reznik. The westward dipoles are identified as "nonlocal modons," that is, vortical cores of stationary nonlinear Rossby waves. In the case of standing Stern modons, some small initial perturbations induce slow westward drift and subsequent collapse of the vortex structure due to the Rossby wave radiation, others lead to their transformation into Larichev and Reznik's modons. This conclusion is supported by the results of a numerical integration of the linear stability problem.

1. Introduction

Dipole mesoscale vortices made their appearance in modern geophysical hydrodynamics some time before they were actually observed in the ocean or atmosphere (Stern, 1975; Larichev and Reznik, 1976). The accession of high-resolution remote sensing imaging devices has made it possible to discover mesoscale vortical pairs in different parts of the World Ocean (Thomson, 1984; Ikeda *et al.,* 1984; Ikeda and Emery, 1985; Kennelly *et al.,* 1985; Ahlnas *et al.,* 1987; Johannessen *et al.,* 1989; Hooker *et al.,* 1995a,b). Stern (1975) suggested the term "modon" to designate a dipole current system described by an exact solution of the equation of conservation of potential vorticity in a barotropic ocean with a plane bottom (i.e., where motions are horizontal) on the β-plane. This solution was constructed by dividing the (x, y)-plane into two parts, a circular area containing two antisymmetric vortices and a motionless exterior, and by matching the internal and the external solutions. Characteristic properties of Stern's modon are zero translation speed and discontinuity of the acceleration and the vorticity of the fluid particles at the matching contour. Larichev and Reznik (1976) subsequently extended this concept to the case of continuous acceleration and vorticity to achieve solutions characterized by greater smoothness and nonzero translation speed. For brevity, solutions marked by continuous and discontinuous vorticity will be henceforth called high-smooth and low-smooth, respec-

1. Department of Physics, Bar-Ilan University, Ramat-Gan 52900, Israel. ***email: zinovyk@mail.biu.ac.il***

tively. Under the "rigid lid" condition, which is appropriate for mesoscale movements, the modon of Larichev and Reznik propagates toward the east. A number of subsequent analytical researches (Flierl *et al.,* 1980; Berestov, 1979, 1981; Kizner, 1984, 1988, 1997) treating of barotropic, two-layer, or three-dimensional modons were inspired by the pioneering works of Stern (1975) and Larichev and Reznik (1976). Numerically, it was shown that modon-like westward-going dipoles may result from the interaction of isolated barotropic vortices (McWilliams, 1983), while a vortex with an initially purely baroclinic mode structure, in a two-mode model, may behave as an eastward propagating modon (McWilliams and Flierl, 1979). Similarly, Mied and Lindemann (1982), in the framework of a two-layer numerical model, demonstrated that a heton-type pair of vortices, while evolving, creates a dipolar barotropic mode that determines the eastward propagation of the entire vortical structure.

Apart from the dipolar modons, more complicated multipolar structures (in terms of both streamfunction and potential vorticity) with poles located on a straight line parallel to the y-axis can be constructed based on the Stern and Larichev and Reznik solutions. Using numerical techniques, the propagating barotropic modons of Larichev and Reznik have been shown to be quite resistant (McWilliams *et al.,* 1981; see also Makino *et al.,* 1981; Larichev and Reznik, 1982, 1983; McWilliams and Zabusky, 1982). However the robustness of standing Stern modons as well as that of multipolar Stern or Larichev and Reznik solutions, to the best of our knowledge, has not yet been examined in such a way.

In the present paper, the stability properties of Stern's modons and the four-polar solutions of Stern and Larichev-Reznik, which following Orlandi *et al.* (1994) can be called "shielded modons," are studied by means of a high-resolution numerical model. Initial value problems were run with these exact solutions set as initial states. The shielded Stern and Larichev and Reznik modons were found to be unstable. Larichev and Reznik's shielded modon collapses within a few synoptic periods (i.e., about a month). Stern's shielded modon persists longer, but ultimately also collapses. A remarkable outcome of the experiments with these solutions is the finding that vortical pairs traveling nearly steadily west and east are emitted at a certain stage of evolution. This has something in common with the numerical results of Orlandi *et al.* (1994) and Hesthaven *et al.* (1995). They studied two-dimensional shielded dipoles in a uniformly rotating fluid, that is, within the f-plane approximation, which may be appropriate for small-scale vortices. Orlandi *et al.* proved instability of Lamb's (1932) shielded modon, while Hesthaven *et al.* demonstrated the transformation of the core part of a shielded dipole categorized by a cubic relationship between the potential vorticity and the streamfunction into a nonshielded dipole. However, β-effect plays a significant role in the dynamics of synoptic eddies in the ocean (Kamenkovich *et al.,* 1986), which we are addressing in the present work.

Reliable identification of the emitted quasi-stable structures in terms of exact solutions is made difficult by their relatively small sizes. Nonetheless, we attach much importance to this result, which was typical for most of our experiments with different kinds of unstable vortex structures. This is why much of the present study is focused on the evolution of compact vortex structures that, in the course of this evolution, radiate eastward and westward propagating dipoles large enough to be reliably identified. In terms of the streamfunction, the initial states in the corresponding runs are made up of dipoles positioned in a motionless fluid, but due to the high smoothness of the streamfunction, they are of a four-polar character when considered from the viewpoint of potential vorticity. It should be observed that, in our numerical simulations, not only the internal vortices transformed into unshielded dipoles, but also their break-away "shields" usually joined together to form a dipolar structure. The emerged eastward eddy pair is shown to be Larichev and Reznik's modon, while the westward dipole is identified as the core of a quasi-stationary nonlinear Rossby wave characterized by a linear relationship between the potential vorticity and the streamfunction (taken in the traveling frame) in the inner area, which is in fact the so-called "nonlocal modon" (Boyd, 1994). The westward modon also shows some degree of similarity to the strongly nonlinear modon studied by Flierl and Haines (1994), but represents a high-smoothness exact solution, possesses a more complicated external structure and allows greater freedom in the choice of parameters.

Immediate interpretation of the evolutionary experiments with Stern's modon is somewhat complicated due to the numerical effects, which decrease as the resolution of the model increases. Based on a comparative analysis of the results obtained at different resolutions, we arrived at the conclusion that such structures are unstable, their evolution being dependent on the type of perturbations imposed on the initial state. Some small initial perturbations induce slow westward drift and subsequent collapse of the vortex structure due to Rossby wave radiation, while others cause Stern's modon to transform into a Larichev and Reznik's modon that travels eastward. Results of a numerical integration of the linearized equation governing the evolution of an initial perturbation imposed upon the Stern modon support the conclusion regarding its instability (or feeble stability).

Our experiments suggest that, along with the conventional Rossby wave radiation, the emergence of long-lived eastward and westward propagating modons is a typical outcome of the evolution of unstable barotropic vortex structures on the β-plane. Thus the results presented below add to our understanding of the abundance of paired vortices in the ocean.

2. Equations and initial conditions

We will base our consideration on the well-known law of conservation of potential vorticity. When a barotropic ocean on the β-plane with a plane bottom is considered and the "rigid lid" condition is assumed at the upper surface, the potential vorticity is given by

$$\zeta = \nabla^2\psi + \beta y, \tag{1}$$

while the conservation equation is

$$\frac{\partial \zeta}{\partial t} + \frac{\partial \psi}{\partial x}\frac{\partial \zeta}{\partial y} - \frac{\partial \psi}{\partial y}\frac{\partial \zeta}{\partial x} = 0 \tag{2}$$

or

$$\frac{\partial}{\partial t}\nabla^2\psi + \beta\frac{\partial\psi}{\partial x} + \frac{\partial(\psi, \nabla^2\psi)}{\partial(x, y)} = 0. \tag{3}$$

Here x and y are the eastward and northward coordinates, ψ is the streamfunction $\beta =$ const. is the northward gradient of the Coriolis frequency, ∇^2 and $\partial/\partial(x, y)$ are Laplacian and Jacobian operators in x, y.

To set an initial value problem, it is necessary to specify the initial and boundary conditions. The initial states under consideration are discussed below in this section, while the boundary conditions applied in the numerical model are described in Section 3. The exact steady-state solutions of Eq. (3) suggested by Stern (1975) and Larichev and Reznik (1976) constitute an important class of initial conditions. The vortices specified by these solutions may stand (Stern), or they may propagate eastward (Larichev and Reznik) at a constant translation speed s without changing structure. In the moving reference frame, $\xi = x - st$, y, associated with such a steady vortex, Eq. (3) is replaced with

$$\frac{\partial}{\partial(\xi, y)}[\psi + sy, \nabla^2\psi + \beta y] = 0, \tag{4}$$

where the differentiation is carried out with respect to ξ instead of x. The meaning of Eq. (4) is that, in the moving reference frame, the potential vorticity, ζ, is conserved along the streamlines, i.e., is an arbitrary function of the full streamfunction, $\Psi = \psi + sy$.

Using the polar coordinates r, α defined by $\xi = r\cos\alpha$, $y = r\sin\alpha$, Stern's solution of Eq. (4) and that of Larichev and Reznik can be represented by a unified formula:

$$\psi = \begin{cases} \left[AJ_1(pr) - \left(\dfrac{\beta}{p^2} + s\right)r\right]\sin\alpha, & r < r_0, \\ BK_1(qr)\sin\alpha, & r > r_0, \end{cases} \tag{5}$$

where J_1 and K_1 are the first-order Bessel and Macdonald functions, respectively, p, q and r_0 are constants, $A = \beta r_0/[p^2 J_1(pr_0)]$. Zero values of the parameters s and B correspond to the standing solution of Stern, while the relationships $s = \beta/q^2 > 0$ and $B = -\beta r_0/[q^2 K_1(qr_0)]$ determine the eastward propagating solution of Larichev and Reznik. In Stern's solution both the streamfunction and the velocity fields are continuous but the vorticity is discontinuous at the separatrix contour $r = r_0$ (at which $\Psi = 0$), whereas in that of Larichev and Reznik the vorticity field is continuous (high smoothness). Correspondingly, in Stern's solution the matching conditions require that $J_2(pr_0) = 0$, while in Larichev and Reznik's solution they give the so-called dispersion relationship for Rossby solitons that relates the parameters $\kappa = pr_0$ and $\lambda = qr_0$:

$$-\kappa\frac{J_1(\kappa)}{J_2(\kappa)} = \lambda\frac{K_1(\lambda)}{K_2(\lambda)}, \tag{6}$$

where J_2 and K_2 are the second-order Bessel and Macdonald functions, respectively.

Conventionally, in the case $s = 0$, the first zero of the equation $J_2(pr_0) = 0$ is chosen, $pr_0 = j_{2,1} \approx 5.136$, to yield the classical dipolar standing modon (Stern, 1975). Similarly, a moving dipolar modon is obtained if κ in Eq. (6) ranges within the first zeros of the functions J_1 and J_2, that is, if $3.832 \approx j_{1,1} < \kappa < j_{2,1} \approx 5.136$ (Larichev and Reznik, 1976). However, the solution (5) describes multi-polar structures as well. If, say, one puts $s = 0$ and $pr_0 = j_{2,2} \approx 8.417$, or $s > 0$ and $7.016 \approx j_{1,2} < \kappa < j_{2,2} \approx 8.417$, then a shielded modon, that is, a structure comprising four vortices, respectively standing or moving, will be obtained.

In the numerical experiments described below, we examine the evolution of such shielded modons, as well as that of a dipolar Stern modon, and show that the shielded modons are unstable. An interesting manifestation of this instability is the emission of vortex dipoles that travel both eastward and westward (Section 4). The relatively small size of these dipoles, however, makes it difficult to identify them in terms of exact solutions of Eq. (3) or (4). In order to ascertain to what degree such dipole generation is typical, and to facilitate the identification of emerging vortical pairs, we consider the evolution of vortex configurations that do not represent an exact steady-state solution but merely serve as initial conditions for the model runs. These initial states are given by the function

$$\psi|_{t=0} = \begin{cases} a[J_1(br) + cr^3 + dr] \sin \alpha, & r < r_0, \\ 0, & r > r_0, \end{cases} \tag{7}$$

where the parameters b, c and d are fitted so as to assure the continuity of the streamfunction, velocity, and vorticity fields. The amplitude factor a remains arbitrary and can be taken to be both positive and negative. This implies that Eq. (7) can be utilized to describe not only shielded dipole structures akin to the shielded modons given by Eq. (5), but structures made up of inverse vortices as well. Note that the vorticity field given by (7) can be four-polar even if the streamfunction has only two poles.

Effects specific to numerical models require especially careful execution and scrutiny of the experiments for the case of standing solutions or small translation speeds. That is why we will begin by demonstrating the instability of the shielded modons of Larichev and Reznik in Subsection 4a below, then go on to study the evolution of structures given by Eq. (7) (Subsection 4b), and only after that the stability properties and evolution of Stern's modons will be discussed in Subsection 4c.

3. Numerical model

The numerical model was developed based on the principle of conservation of potential vorticity. A number of initial value problems were integrated with the configurations (5) and (7) set as initial states. We used nondimensional versions of Eqs. (1), (2), (5), (7) with the scales L and $T = 1/\beta L$ for the space and time variables, and $\psi^* = \beta L^3$ and $\zeta^* = \beta L$ for the streamfunction and vorticity, respectively. In the most of the experiments, a square $15L \times 15L$ grid with the mesh size $\delta = 0.1L$ was considered. In the course of the computations the time step τ was controlled by the gradients of ψ and ζ and did not exceed

$2.5 \cdot 10^{-3}T$. The boundary conditions assumed were periodicity in the x-direction and $\psi = 0$ at the northern and southern boundaries.

Briefly, the computational algorithm is as follows. At any moment $t > 0$ the vorticity is computed from a finite analog of Eq. (2) with the use of a combination of direct and Matsuno schemes and the Arakawa approximation for the Jacobian operator (Mezinger and Arakawa, 1976), which affords conservation of the integral vorticity, the streamfunction being taken from the previous moment, $t - \tau$. Subsequently, ψ is determined as a solution of the Poisson problem (1), using a decomposition into eigenfunctions in the x-direction and a sweep method in the y-direction (Samarsky, 1989).

The Larichev and Reznik modons moving east with the translation speeds 0.3 to $1.2L/T$ were used to test our model. No visible changes in their structures were registered within a period of $300T$. Subsequently, experiments were run with the initial states described above. Conservation of total energy and enstrophy was found to hold within 0.1 to 0.3% in all our experiments.

As we are dealing with nondimensional variables, henceforth the scales T, L, L/T, L^{-1} etc. will be omitted unless essential for clarity. Even though in our nondimensional model $\beta = 1$, the symbol β will be retained in all relevant relations in order to set off the role of the β-effect.

4. Results and discussion

Below we present the results of numerical experiments relating to the evolution of the vortex structures generated at $t = 0$ by Eqs. (5) and (7).

a. Instability of the Larichev and Reznik shielded modon

In contrast with the conventional Larichev and Reznik modons, the shielded modons given by Eqs. (5) and (6) exhibited strong instability in our computer simulations, collapsing within a few synoptic periods. The evolution of a Larichev and Reznik shielded modon determined by the parameters $r_0 = 1.5$ and $s = 0.8$ (that is, $k = 4.754$, $\kappa = 7.131$) is shown in Figure 1. In terms of ζ-contours, the instability manifests itself in a gradual breaking away of the outer vortices from the central core in the eastward direction, each such vortex splitting into two distinct parts. The eastern parts join, creating a dipole that travels east. In parallel, the core vortices elongate in the x-direction, and, gradually, the greatest vorticity becomes concentrated in their western parts, which by $t = 7$ form a distinct vortex pair moving west. [Note, that formally, due to potential vorticity conservation, which forbids the breaking and closing of ζ-contours (see, e.g., Larichev, 1983a,b), the separated vortices must be connected by some filaments. However, these filaments may thin down so that they cannot be resolved by the numerical model.] The subsequent propagation of each of the two vortical pairs is quite steady, but due to the relatively small size of these dipoles, they cannot be reliably identified in terms of exact solutions of Eq. (3).

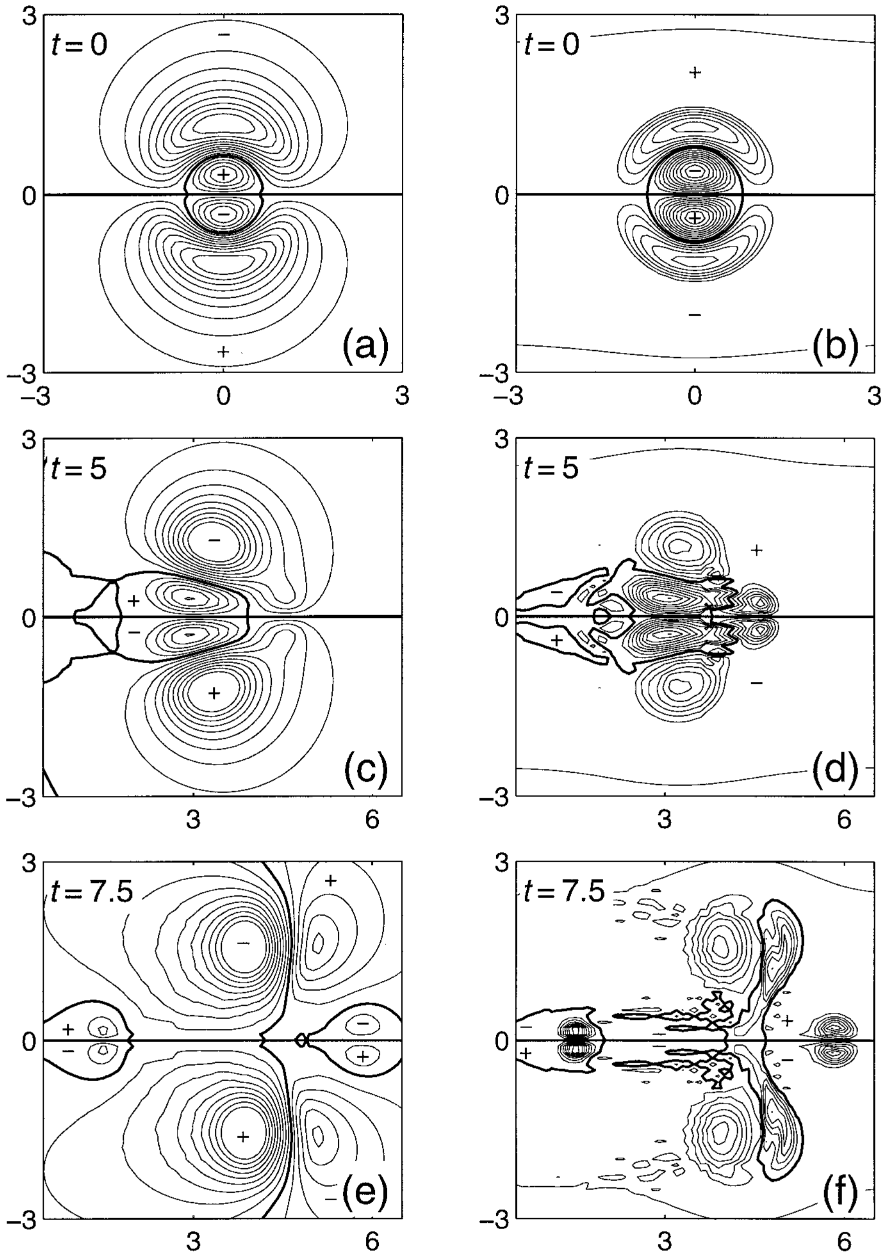

Figure 1. Collapse of the Larichev and Reznik shielded modon given by solution (5), (6) at $r_0 = 1.5$ and $s = 0.8$ in terms of streamfunction (on the left—a, c, e) and potential vorticity (on the right—b, d, f): formation of the eastward and westward modons.

b. Modon emission from nonstationary shielded dipole structures

i. Overview. When experimenting with the structures given by Eq. (7), two cases, $a = -2.5$ and $a = 2.5$, were considered, in the both experiments the values $r_0 = 1.5$, $b = 4.253$, $c = 0.282$ and $d = 0.759$ being used. The corresponding results are presented in Figs. 2–9 and are discussed below; the initial states are shown in Figures 2a,b and 5a,b. According to our computations, these structures collapse within the synoptic period T (Figs. 2, 5, 6a,b). The two experiments at $a < 0$ and $a > 0$, below referred to as the first and the second, respectively, share the common property that the decaying structures radiate vortical pairs traveling both east and west. These radiated dipoles exhibit relative stationarity (Figs. 3, 6, 7a, 8a, 9a) and high smoothness (Figs. 7d, e, 8d, e, 9d, e) and are strong enough to survive in interactions that occur due to the periodicity assumed in our model (Figs. 4).

ii. Quasi-stationarity. As noted above, when a form-preserving structure propagates in the x-direction with constant speed U, its potential vorticity ζ functionally depends on the streamfunction $\Psi = \psi + Uy$ in the moving reference frame $\xi = x - Ut$, y. According to (4), if this structure is compact, that is if $\psi \to 0$ and $\nabla^2\psi \to 0$ at $r \to \infty$, then at sufficiently large r that dependence must be a simple proportionality, $\zeta = \pm l^2\Psi$, implying that $\nabla^2\psi = \pm l^2\psi$, where $l^2 = \pm\beta/U = \text{const}$. This immediately supplies a number of criteria for testing the stationarity of the generated vortical pairs. First, if such a dipole is already formed and propagates steadily (or evolves slowly with a characteristic time of change considerably exceeding T), then its apparent translation speed U must stabilize. Second, away from the dipole core, the proportionality between the relative vorticity and the streamfunction, $\nabla^2\psi \approx \pm l^2\psi$, must be good. Finally, the translation speed, $\tilde{U} = \beta/\pm l^2$, estimated using the above factor of proportionality $\pm l^2$, must conform with the estimate U obtained by analysis of the displacements of the vortices (Figs. 7a, 8a and 9a).

Based on these criteria and according to our estimates, the outer parts of the generated dipole structures can be regarded as quasi-stationary or evolving very slowly (Figs. 7a,b; 8a,b and 9a,b). In the first experiment (at $a < 0$), the visible speed of propagation of the right-hand (eastward) dipole stabilizes at $t \approx 3$ and remains nearly constant ($U \approx 1.89$) until $t \approx 7$ (Fig. 7a), at which time the interaction between the eastward and westward dipoles starts (Fig. 4a,b); so any t within the interval $3 < t < 7$ can be chosen for testing. For example, at $t = 3$ the correlation between $\nabla^2\psi$ and ψ (Fig. 7b) is good, the coefficient of correlation R being extremely high ($R \approx 0.9998$), and the two estimates of the translation speed are in close agreement ($\tilde{U} \approx 1.93$ versus $U \approx 1.89$). The left-hand (westward) dipole in this experiment is weaker and less stable; the corresponding estimates are: $U \approx -0.83$ (average over the period from $t = 4.4$ to $t = 7$), $\tilde{U} \approx -0.69$ (at $t = 6$), $R \approx -0.9996$ (Fig. 8b). In the second experiment (where $a > 0$), the generated westward dipole shapes at $t \approx 2.75$ and remains nearly stable until $t \approx 6$. The estimates of its translation speed are $U \approx -2.20$ and $\tilde{U} \approx -2.33$ (at $t = 2.5$), the coefficient of correlation being $R = -0.9997$. The second of the dipoles generated in this experiment shifts to the east very slowly and, in

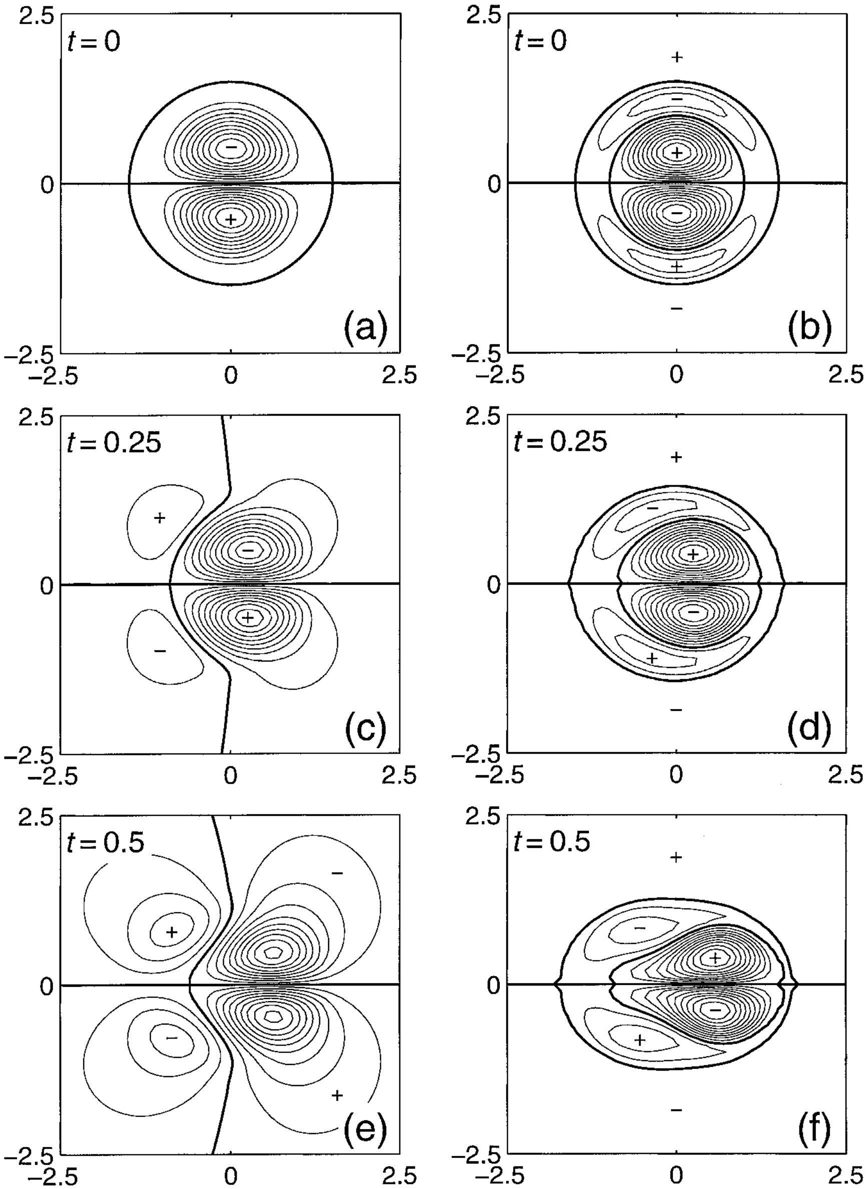

Figure 2. Initial stage of evolution of the structure given by Eq. (7) at $a = -2.5$ and $r_0 = 1.5$ in terms of streamfunction (on the left—a, c, e) and potential vorticity (on the right—b, d, f): formation of the eastward and westward modons.

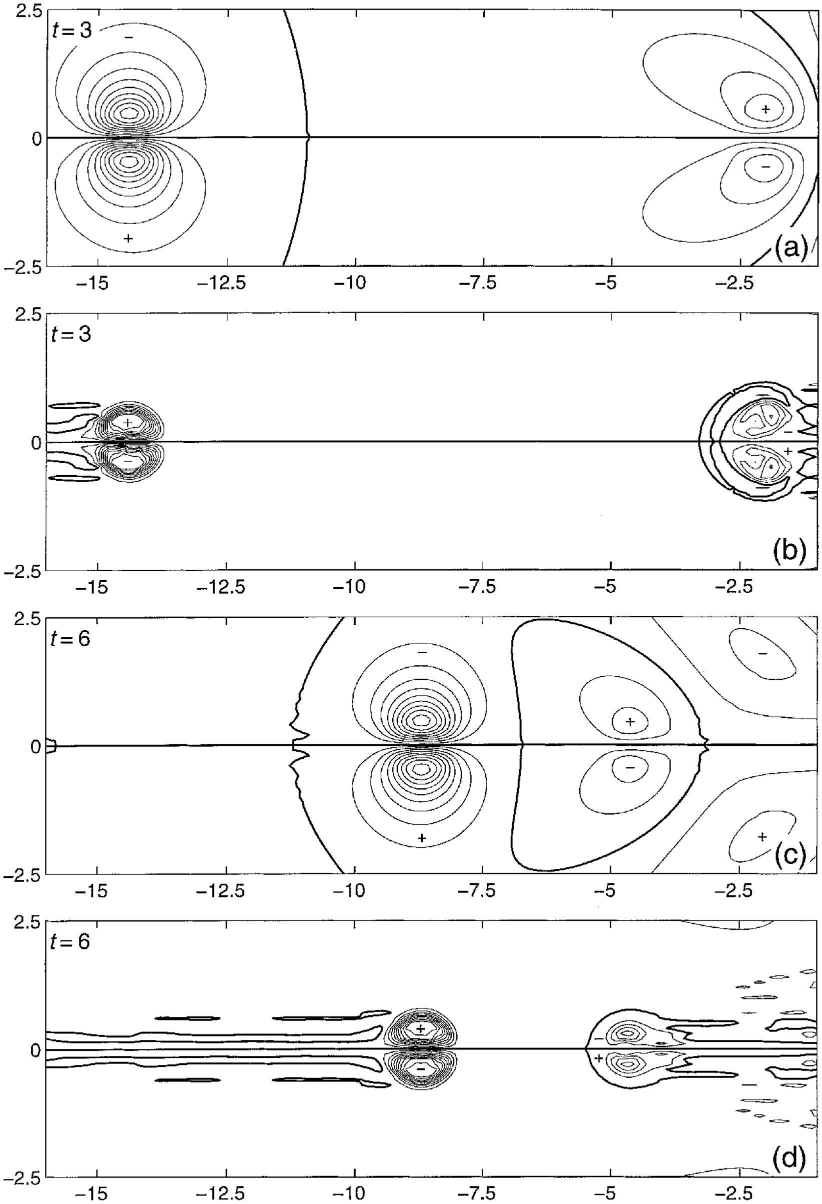

Figure 3. Quasi-steady propagation of the eastward and westward modons resulting from collapse of the structure determined by (7) at $a = -2.5$ and $r_0 = 1.5$ (Fig. 2a, b): streamfunction (a, c) and potential vorticity (b, d).

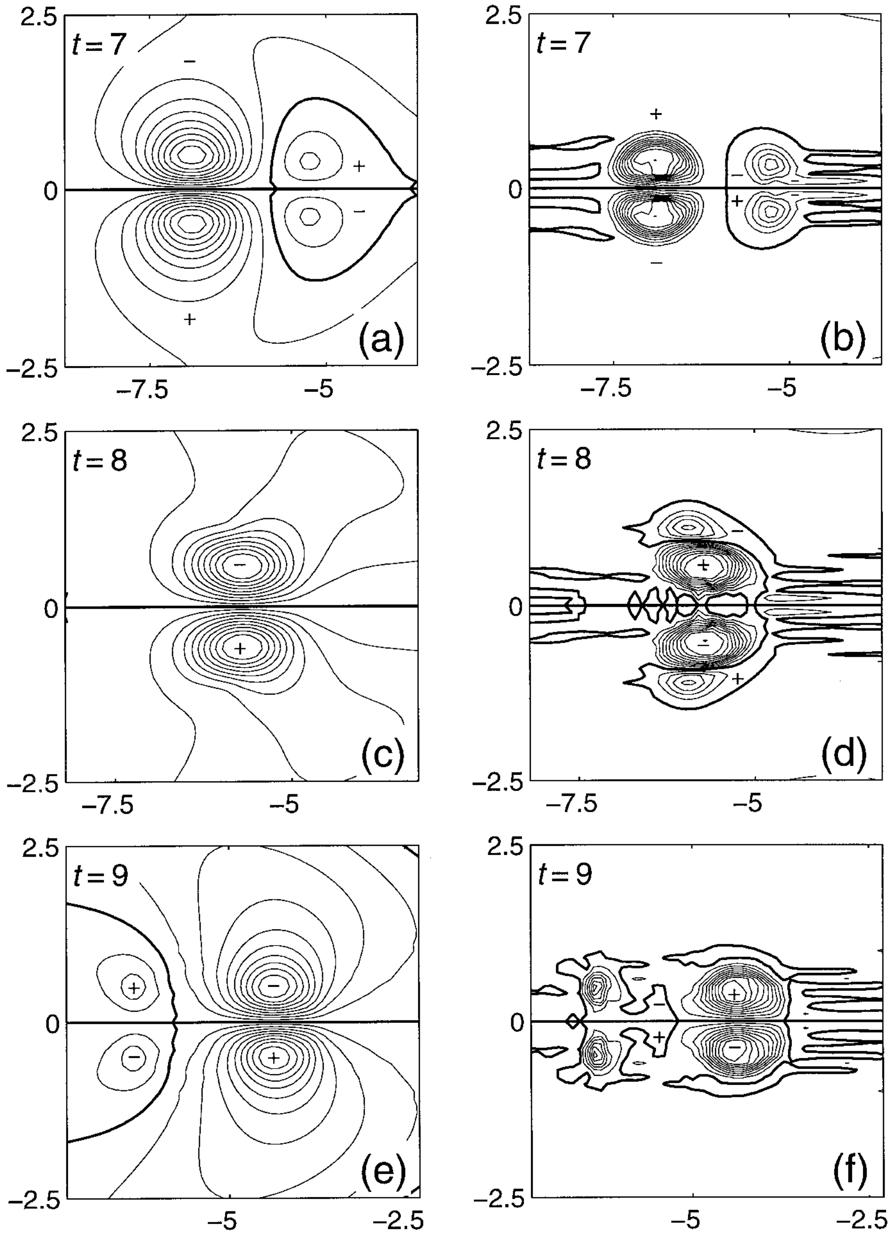

Figure 4. Late stage of evolution of the structure given by (7) at $a = -2.5$ and $r_0 = 1.5$ in terms of streamfunction (on the left—a, c, e) and potential vorticity (on the right—b, d, f): collision of the westward and eastward dipoles.

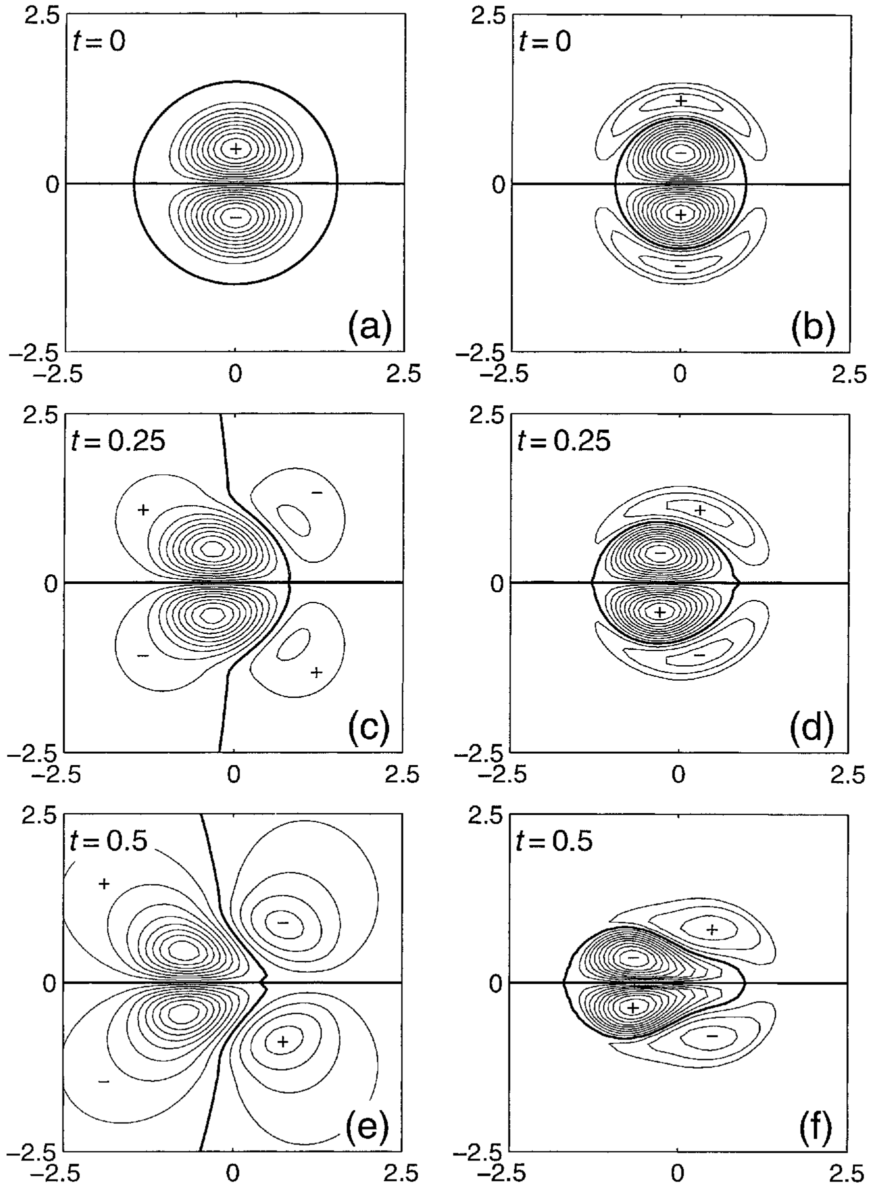

Figure 5. Initial stage of evolution of the structure given by Eq. (7) at $a = 2.5$ and $r_0 = 1.5$ in terms of streamfunction (on the left—a, c, e) and potential vorticity (on the right—b, d, f): formation of the eastward and westward dipoles.

terms of ζ, is not organized well enough to be analyzed and identified in such a manner (Fig. 6). That is why the corresponding estimates are not presented.

In the both experiments under consideration the proportionality established between $\nabla^2\psi$ and ψ holds outside the dipole core right up to the contour of zero Ψ, which indicates

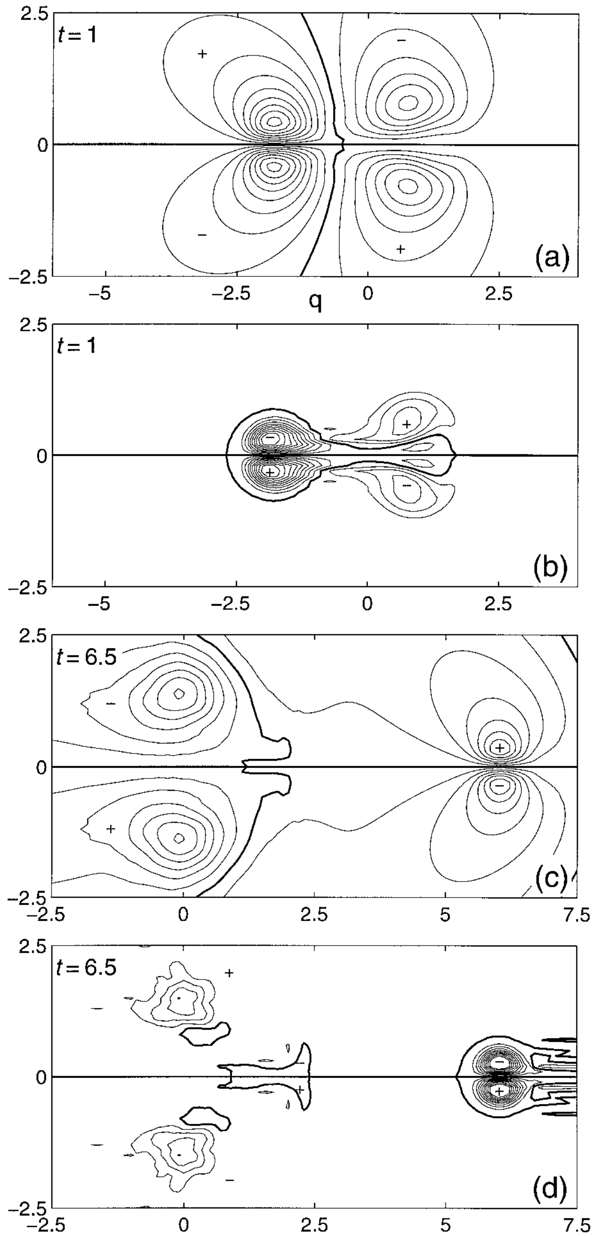

Figure 6. Development and quasi-steady propagation of the westward dipole resulting from collapse of the structure determined by (7) at $a = 2.5$ and $r_0 = 1.5$ (Fig. 5a, b): streamfunction (a, c) and potential vorticity (b, d).

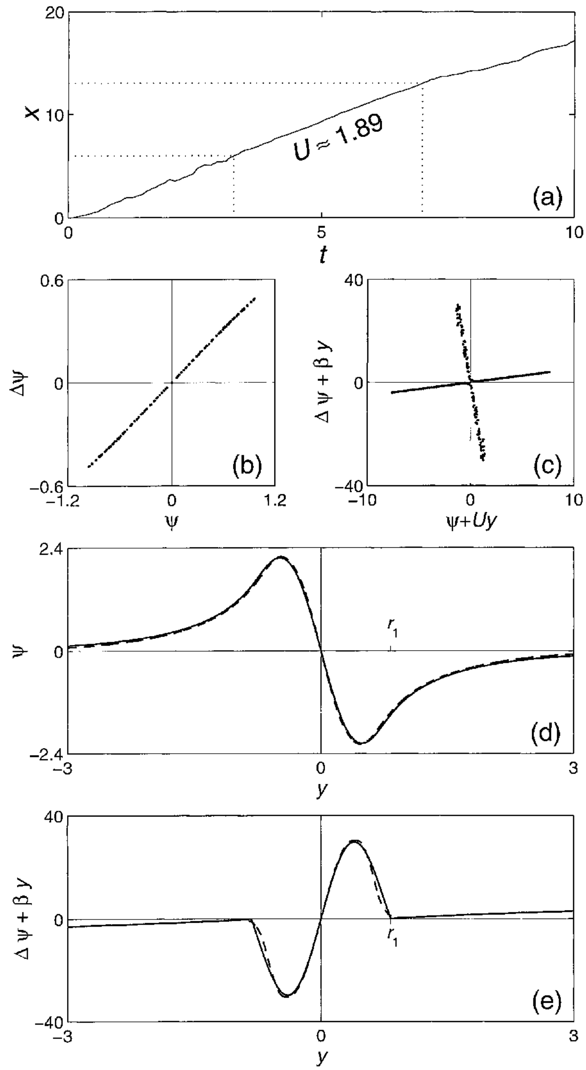

Figure 7. Identification of the eastward modon resulting from collapse of the structure given by (7) at $a = -2.5$ and $r_0 = 1.5$ (Fig. 2a, b): the x-coordinate of max ζ vs. time (a); correlation between $\nabla^2\psi$ and ψ (b): scatter diagram of ζ vs. Ψ (c); computed solution (dashed line) and fitted exact solution (5), (6) (solid line) in terms of streamfunction (d) and potential vorticity (e).

the boundary of the core and is roughly circular. Our estimates of l^2 and $\tilde{U}$ correspond to the annular areas $1.05r_1 < r < 2r_1$, where $r_1 = \text{const.}$ designates the radius of the contour $\Psi = 0$. Note that for the westward vortex pairs the coefficient l^2 bears a minus sign, while in the case of the eastward dipole the correlation is positive.

Clearly, the above criteria are insufficient: in order to judge whether the radiated dipoles

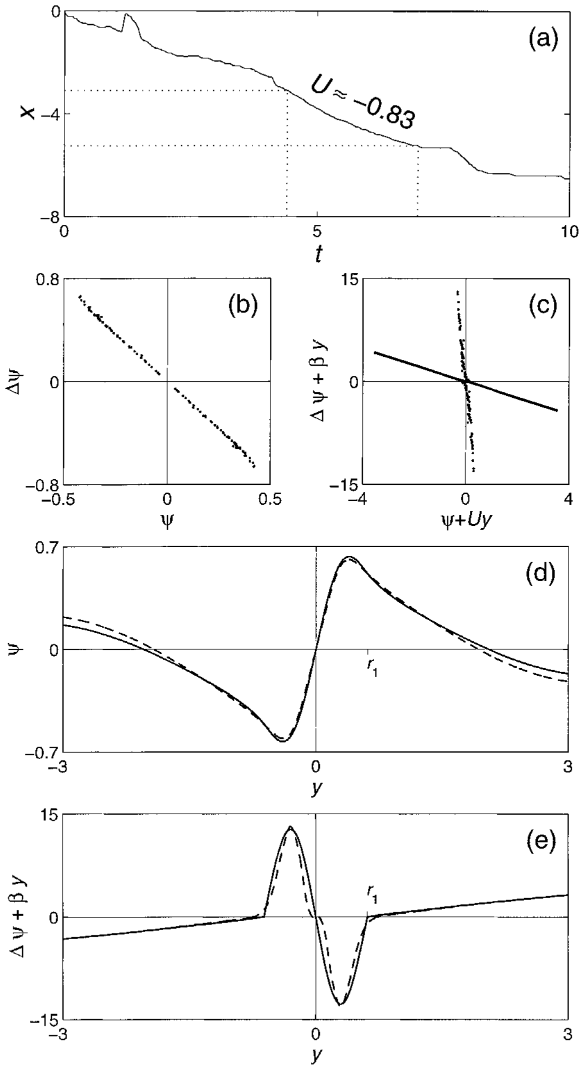

Figure 8. Identification of the westward modon resulting from collapse of the structure given by (7) at $a = -2.5$ and $r_0 = 1.5$ (Fig. 2a, b): the x-coordinate of min ζ vs. time (a); correlation between $\nabla^2\psi$ and ψ (b); scatter diagram of ζ vs. Ψ (c); computed solution (dashed line) and fitted exact solution (8) (solid line) in terms of streamfunction (d) and potential vorticity (e).

can be regarded as stationary or not, we have to test how closely $\zeta = \nabla^2\psi + \beta y$ and $\Psi = \psi + Uy$ are related in the interior, i.e., within the contour $\Psi = 0$. The scatter-diagrams of ζ vs. Ψ shown in Figures 7c, 8c and 9c indicate quite a good correlation between potential vorticity and streamfunction (taken in the moving reference frame) in both the exterior and interior regions, the coefficients of correlation for the interior being -0.9919, -0.9884 and

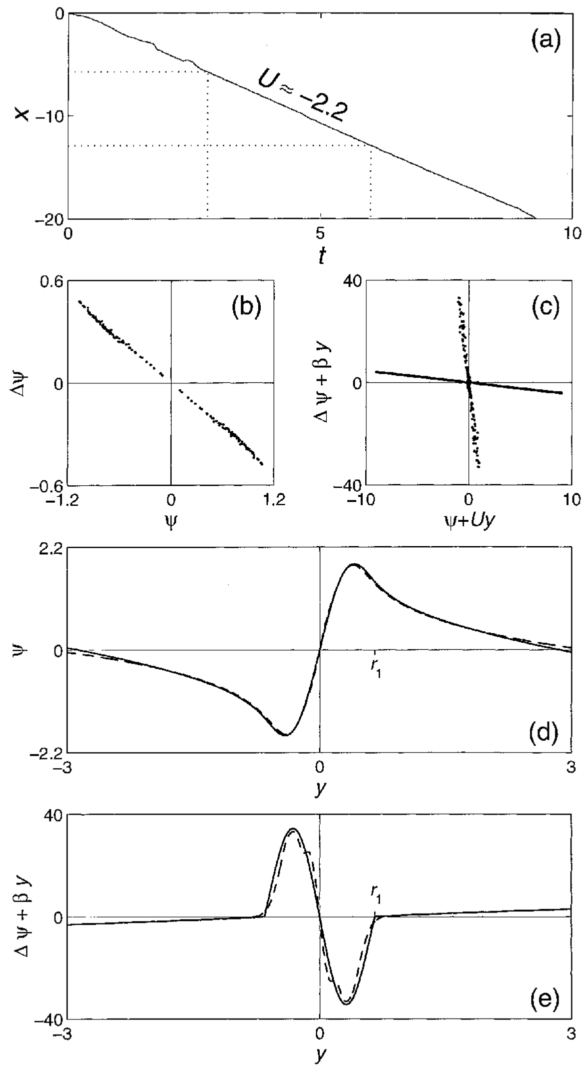

Figure 9. Identification of the westward modon resulting from collapse of the structure given by (7) at $a = 2.5$ and $r_0 = 1.5$ (Fig. 5a,b): the x-coordinate of min ζ vs. time (a); correlation between $\nabla^2\psi$ and ψ (b); scatter diagram of ζ vs. Ψ (c); computed solution (dashed line) and fitted exact solution (8) (solid line) in terms of streamfunction (d) and potential vorticity (e).

-0.9833, respectively. This means that, within the contour $\Psi = 0$, the proportionality $\zeta = -k^2\Psi$ is valid to a high level of approximation. For the eastward vortex pair $k \approx 4.78$. For the westward dipole $k \approx 5.19$ in the first experiment and $k \approx 5.77$ in the second. The quasi-steady eastward- and westward-propagating dipoles generated in the two experiments are shown in Figures 3 and 6.

iii. Identification of dipoles. If we neglect the small changes in U, ζ and Ψ that take place at the stages of quasi-steady propagation of the radiated dipoles, then the following question arises: what high-smoothness exact solutions of Eq. (4) can describe the structure and dynamics of these vortex pairs that have essentially continuous fields of streamfunction, velocity and vorticity?

Based on our analysis, in the case of the eastward dipole (the first experiment) we have the equation:

$$\nabla^2\psi + \beta y = \begin{cases} -k^2(\psi + Uy), & r < r_1, \\ l^2(\psi + Uy), & r > r_1, \end{cases}$$

which yields the familiar Larichev and Reznik modon given by Eqs. (5) and (6), where p, q and r_0 are replaced with k, l and r_1, respectively, A and B are functions of k, l and r_1; $\lambda = lr_1$ and $3.832 \approx j_{1,1} < \kappa = kr_1 < j_{2,1} \approx 5.136$. An exact solution of this type can be fitted to the eastward dipole.

The correspondence between actual ψ and ζ at $t = 3$, on the one hand, and the fitted exact solution (5), (6) on the other, is evident from Figure 7d,e. The fitting was carried out for the meridional cross section passing through the points of maximum and minimum of ψ and ζ by minimization of the integral (over the interval $-2r_1 < y < 2r_1$) squared deviation, *ISD*, of the theoretical ψ from the actual one. In the minimization procedure, *ISD* was regarded as a function of r_1 and U, while parameter k was determined from relationship (6), where $\lambda = r_1 l = r_1\sqrt{\beta/U}$. The found "best fit" estimates of r_1, U and k, ($r_1 = 0.83$, $U = 1.80$ and $k = 4.67$) are quite close to the observed radius of the zero Ψ contour ($r_1 = 0.82$) and the above estimates of U and k, attesting to that our eastward dipole does indeed belong to the category of Rossby solitions described by Larichev and Reznik (1976).

The nature of the westward vortex pairs can be established in a similar manner. For these structures we have the following equation:

$$\nabla^2\psi + \beta y = \begin{cases} -k^2(\psi + Uy), & r < r_1, \\ -l^2(\psi + Uy), & r > r_1. \end{cases}$$

Its general solution, which is limited at $r = 0$ and has continuous streamfunction, velocity and vorticity, can be expressed in terms of the first-order Bessel and Neumann functions J_1 and N_1:

$$\psi = \begin{cases} \left[AJ_1(kr) - \left(\dfrac{\beta}{k^2} + U\right)r\right]\sin\alpha, & r < r_1, \\ [BJ_1(lr) + CN_1(lr)]\sin\alpha, & r > r_1. \end{cases} \tag{8}$$

The coefficients A, B and C determined by the conditions of matching ψ, $\partial\psi/\partial r$ and $\partial^2\psi/\partial r^2$ at $r = r_1$ are functions of r_1, l and k:

$$A = \frac{\beta r_1}{k^2 J_1(kr_1)},$$

$$B = \frac{A}{D}[lJ_2(kr_1)N_1(lr_1) - kJ_1(kr_1)N_2(lr_1)],$$

$$C = \frac{A}{D}[kJ_2(lr_1)J_1(kr_1) - lJ_1(lr_1)J_2(kr_1)],$$

where

$$D = \frac{l^2}{k}[J_2(lr_1)N_1(lr_1) - J_1(lr_1)N_2(lr_1)]$$

and J_2 and N_2 are the second-order Bessel and Neumann functions. It is significant that no "dispersion relationship" is imposed upon the parameters r_1, l and k of the solution (8), and hence they can be taken arbitrarily subject only to the conditions that they be positive and $J_1(kr_1) \neq 0$.

Taking l corresponding to the apparent translation speed ($l = r_1\sqrt{-\beta/U}$) and minimizing *ISD* as a function of both r_1 and k we fitted a solution from (8) to the observed westward dipoles at $t = 6$ (note that l, r_1, and k in (8) are independent). In the first experiment, where $U = -0.83$, the "best fit" parameter estimates are: $r_1 \approx 0.62$ and $k \approx 6.10$; in the second experiment ($U = -2.20$), the "best fit" r_1 and k estimates are 0.66 and 5.77. These estimates correspond well to the observed $r_1 \approx 0.62$ and the regression estimate $k \approx 6.15$, in the first experiment, and $r_1 \approx 0.65$ and $k \approx 5.77$, in the second experiment. The results of fitting exact solutions of the type (8) to the computed ψ and ζ are shown in Figures 8d,e and 9d,e.

The solution given by (8) oscillates and drops off slowly at infinity:

$$\psi \sim -\sqrt{\frac{2}{\pi l r}}\left[B\cos\left(lr - \frac{\pi}{4}\right) + C\sin\left(lr - \frac{\pi}{4}\right)\right]\sin\alpha \qquad \text{at} \qquad r \to \infty,$$

which means that our westward modons are in fact relatively strong vortical cores of nonlinear Rossby waves characterized by a specific nonperiodic, antisymmetric structure. Boyd (1994), who adapted the spherical solutions of Tribbia (1984) and Verkley (1984) to the β-plane, and Flierl and Haines (1994) independently obtained similar "nonlocal" modon solutions with oscillatory "far fields." Boyd introduced a dispersion relationship by maximizing the ratio between the amplitudes of the core and the "far field." Flierl and Haines considered a strongly nonlinear "nonlocal" modon (though with no BJ_1 component in the "far field"). The solution they studied was actually low-smooth, as, due to the asymptotic approach applied, they used the dispersion relationship of Lamb (1932), $J_1(kr_1) = 0$, for a dipole on the *f*-plane.

Two remarks need to be made in the conclusion of this subsection. The validity of the above identifications is limited both in time, due to the slow evolution of the vortices, and space, as the fitting applies only to the area $r < 2r_1$ (see Figs. 7a–e, 8a–e, and 9a–e). For example, solution (8) should be treated as an approximation to the westward-going dipole and its neighborhood rather than to the overall current field (notice that formally, the Rossby wave field present in solution (8) has infinite energy). Moreover, while the proportionality between ζ and Ψ outside the vortex core (i.e., on open isolines of Ψ) can be strictly proven for truly steady, isolated free vortices on the β-plane (Larichev and Reznik, 1976; see also Flierl *et al.,* 1980), the dependence between ζ and Ψ in the region of trapped isolines may be taken arbitrarily. However, for the circular dipole solutions on the β-plane known to date, this dependence is either linear (conventional modons) or weakly nonlinear (asymptotic solutions of Nycander, 1988). In the latter case the dipole is slightly elliptical. Free elliptical dipoles on the *f*-plane were considered by Boyd and Ma (1990) (see also Hesthaven *et al.,* 1995; Nogan *et al.,* 1996). They showed numerically that in order to provide elliptical modons the relationship between $\nabla^2\Psi$ and ψ in the interior must be nonlinear, but this relationship is linear for circular modons. This seems to be true for the β-plane as well: as the above analysis showed, in each of the dipoles that emerged in our experiments, the separatrix, i.e., the contour of demarcation between the internal and external areas (the zero Ψ contour), was nearly circular (the eccentricity being under 0.02) and the internal ζ vs. Ψ dependence was approximately linear. This is also in agreement with the results of Haupt *et al.* (1993) who dealt with numerical equilibrium circular modon solutions in weak symmetric shear flow on the β-plane: for all types of shear studied they found that the diagnosed functional relationship between the streamfunction in the traveling reference frame and the vorticity appeared linear.

As can be seen from Eq. (3) (or (1) and (2)), antisymmetry with respect to the *x*-axis is inherent in ψ and ζ fields at any time if the initial condition possesses such a property. In this connection, evolutionary experiments are of significance, in which small perturbations break the antisymmetry of the vortex configurations (7). We ran a series of such experiments, the perturbations being introduced into the initial condition by tilting the axis of antisymmetry. As previously, the main result was that at early stages, vortical dipoles with nonzero components of westward and eastward drift emerged within a few synoptic periods. Their subsequent evolution was mainly dependent on the initial tilt angle θ (which ranked from 0.1° to 5° in our runs) and the *x*-component U of the initial translation speed of the emerged dipole. In most of the runs we had no way of following the long-term evolution of these emerged vortex pairs due to their interaction, which was caused by the postulated periodicity in the *x*-direction. However, the eastward-traveling dipoles displayed behavior characteristic of Larichev and Reznik, modons: their oscillated trajectories tending to stabilize (Makino *et al.,* 1981; Hesthaven *et al.,* 1993). The evolution of the westward-going dipoles was also qualitatively similar to that of westward-propagating Larichev and Reznik modons in the equivalent-barotropic model (Hesthaven *et al.,* 1993; Nycander, 1992). In a few simulations that we ran with a $30L \times 15L$ grid pulled out in the x-direction, the westward-going dipoles demonstrated oscillatory, unstable behavior generally similar to that of initially westward-propagating Larichev and Reznik modons in the equivalent-barotropic model (Hesthaven *et al.,* 1993; Nycander, 1992). They either turned up into eastward Larichev and Reznik modons or exhibited a tendency to disintegrate after a number of oscillations. For example, at $\theta = 5°$ the duration of reliably determined westward drift was about $9T$ for $U \approx -0.5$ versus $13T$ for $U = -0.3$. At $\theta = 1°$ the corresponding times were $15T$ and $17T$, respectively. Finally, at $\theta = 0.1°$ the westward drift times were around 20–$25T$ both. Thus, the possibility for both eastward and reasonably long-standing westward drift of the emerged vortex pairs can be judged from these experiments.

c. *Evolution of Stern's modons*

A number of experiments with Stern's modon (solution (5) at $s = 0$) were carried out at different grid steps δ, the matching radius being taken as $r_0 = 2.35$. For example, in the experiment at $\delta = 0.1$ (Fig. 10), until approximately $15T$ no significant changes in ψ and ζ fields can be observed (Fig. 10a–d), while within the next $15T$ the vortical pair undergoes a certain deformation and shifts slightly to the west (Fig. 10c–f). At the subsequent stage of evolution the two vortices separate and keep away from each other, their intensities (in terms of the streamfunction) decreasing. In fact, at this stage, a classical scenario was observed: the westward moving eddies that initially constitute a coherent structure lose their energy due to Rossby wave radiation (Larichev, 1983a,b; Flierl, 1987; Nycander, 1994) and gradually drift apart, approaching their "rest latitudes" (Larichev, 1983a,b). Similar results were obtained at other values of the grid step. To summarize them briefly, the smaller the grid step, the slower the observed westward drift of the modon. In other words, this westward drift must be attributed to numerical effects. At the same time, these results suggest instability (or feeble stability) of Stern's modon in the sense that some small but uninterruptedly acting perturbations inducing slow westward drift of the modon may lead to its collapse.

However, the question remains as to whether some evolutionary scenario other than that described above would emerge if the numerical inaccuracies could be minimized. One possible way of overcoming these numerical effects is to run an evolutionary experiment starting from a slightly perturbed initial state. We performed a series of experiments in which the perturbations given by Eq. (7) at $a < 0$ were added to Stern's modon at $t = 0$, the perturbation amplitudes increasing gradually from run to run. While very small perturbations did not change the modon evolution significantly, perturbations of a certain strength induced the modon's eastward propagation. Let ε be the ratio between the perturbation and the exact initial state amplitudes. The threshold value of this ratio, ε_T, that distinguishes between the subsequent eastward and westward drift of the modon depends on the mesh

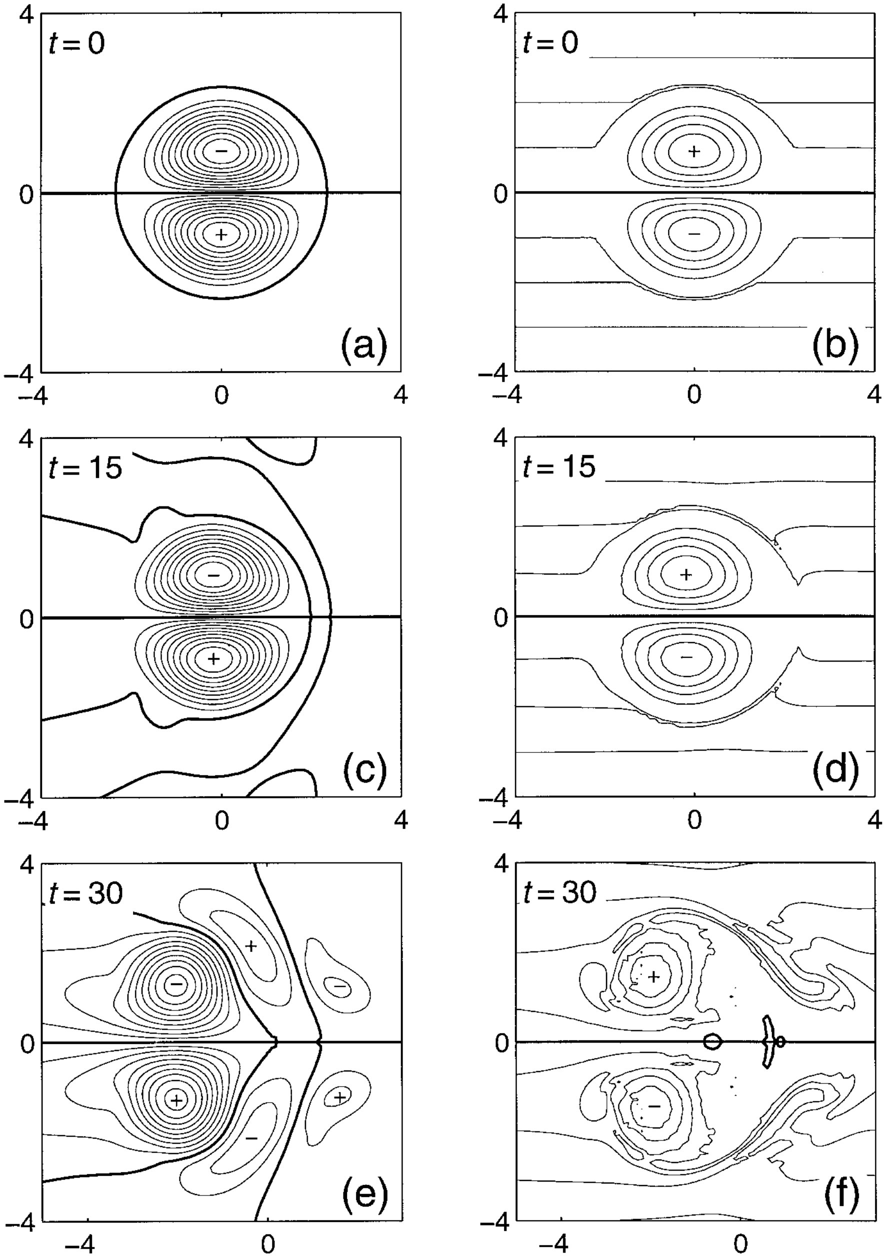

Figure 10. Evolution of the Stern modon (solution (5) at $r_0 = 2.35$ and $s = 0$) at $\delta = 0.1$ resulting from the small perturbations introduced by the numerical scheme: streamfunction (on the left—a, c, e) and potential vorticity (on the right—b, d, f).

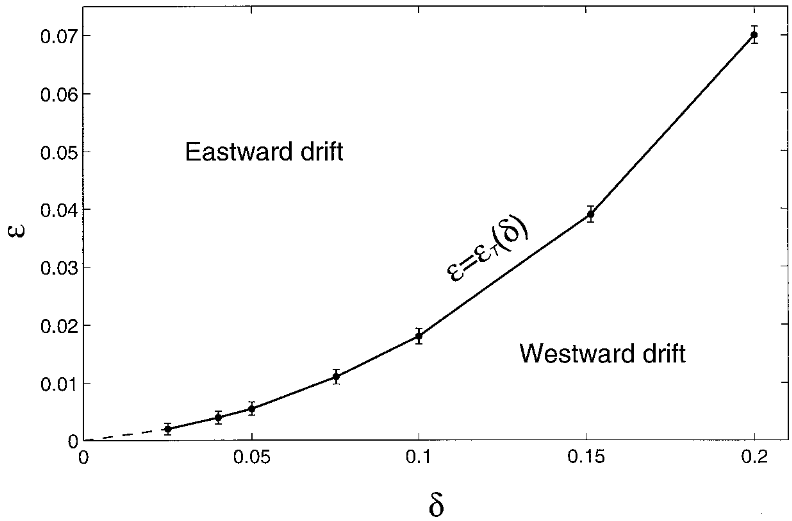

Figure 11. Threshold relative amplitude, ε_T, of the initial perturbation given by (7) at $a < 0$, vs. mesh size, δ, that distinguishes between the subsequent eastward and westward drift of Stern's modon: points—experimental data, bars—possible errors in determining ε_T.

size δ and, based on our data, tends to zero at $\delta \to 0$ (Fig. 11). This result lends support to the above conclusion on the instability of Stern's modon. For example, at $\delta = 0.1$ and $\varepsilon = 0.025$ (Figs. 12, 13) the modon rearranges its outer structure due to smoothing ζ-field (which effect was quite weak in the experiment described above). This can be seen in Figs. 12b,d,f and 13e (cf. Fig. 10b,d,f). The vortex pair does not shift significantly by $t = 25$ (Fig. 12c,d) but constantly accelerates in the eastward direction, picking up a significant eastward speed ($U = 0.092$) which remains nearly constant between $t = 30$ and $t = 50$, the end of the experiment (Fig. 13a). According to our identification criteria (see Subsection 4b and Fig. 13b–e), Stern's modon completes its evolution into a Larichev and Reznik modon ($r_1 = 1.92$, $U = 0.092$) by $t = 30$, and thereafter it propagates almost steadily. The identification of this modon presented in Figure 13 corresponds to $t = 40$, the differences in the estimates obtained by different methods (analysis of the modon drift, scatter diagrams, best fitting) being negligible.

The introduction of a small perturbation in the form (7) at $a > 0$ into Stern's modon leads to westward drift of the vortex structure and its subsequent collapse. This development is similar to, but faster than, that shown in Figure 10.

The experiments presented in this subsection concern instability of Stern's modon to perturbations of finite, even if small, amplitudes. Let us now go over to the examination of its linear stability. For this purpose we will represent the streamfunction ψ in the form $\psi = \psi_S + \varphi$ where ψ_S is the basic solution of Stern and φ is its perturbation. Correspondingly, the potential vorticity ζ is represented as $\zeta = \zeta_S + \omega$, where ζ_S is the potential vorticity of Stern's modon and

$$\omega = \nabla^2\varphi \tag{9}$$

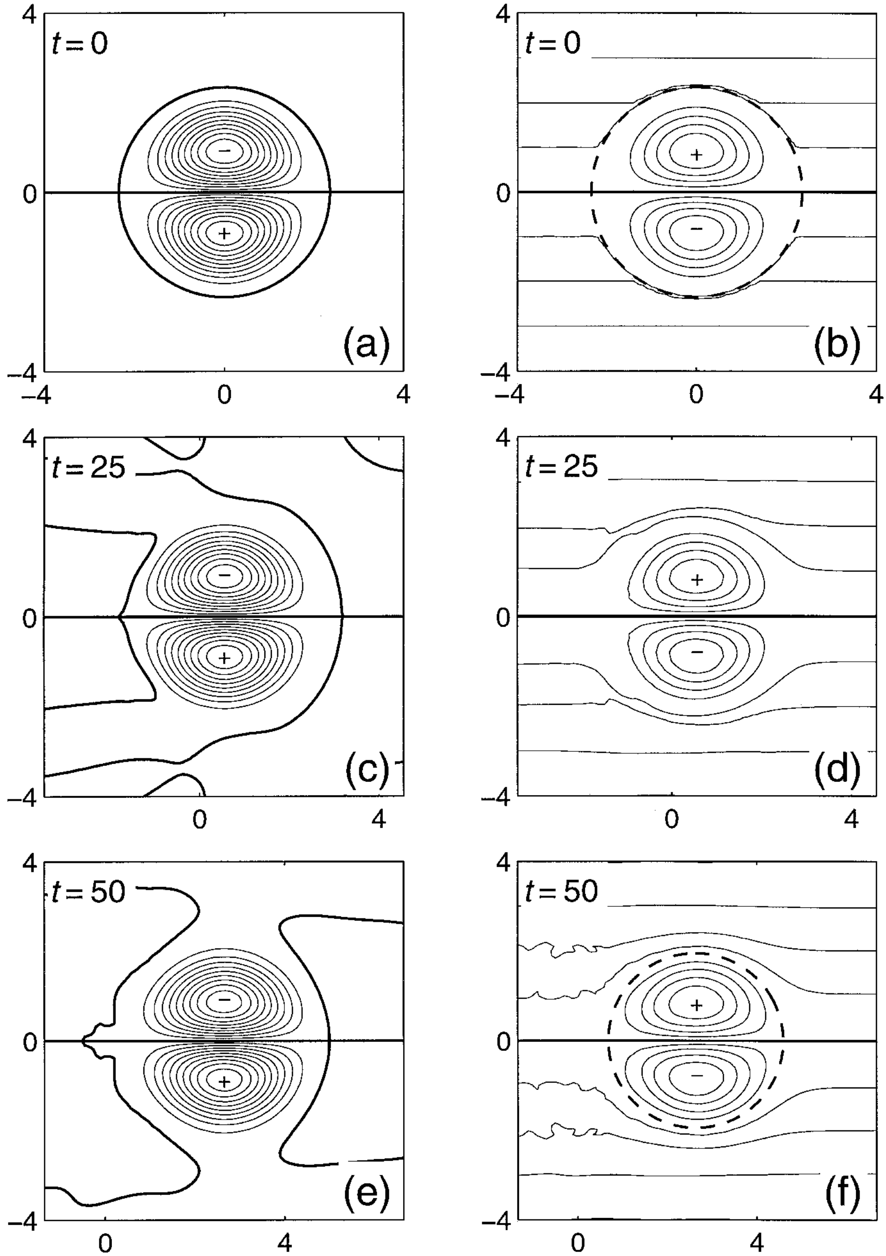

Figure 12. Transformation of the Stern modon (solution (5) at $r_0 = 2.35$ and $s = 0$) into a Larichev and Reznik modon resulting from the addition of a small perturbation in the form (7) to the initial state ($\delta = 0.1$, $\varepsilon = 0.025$): streamfunction (on the left—a, c, e) and potential vorticity (on the right—b, d, f).

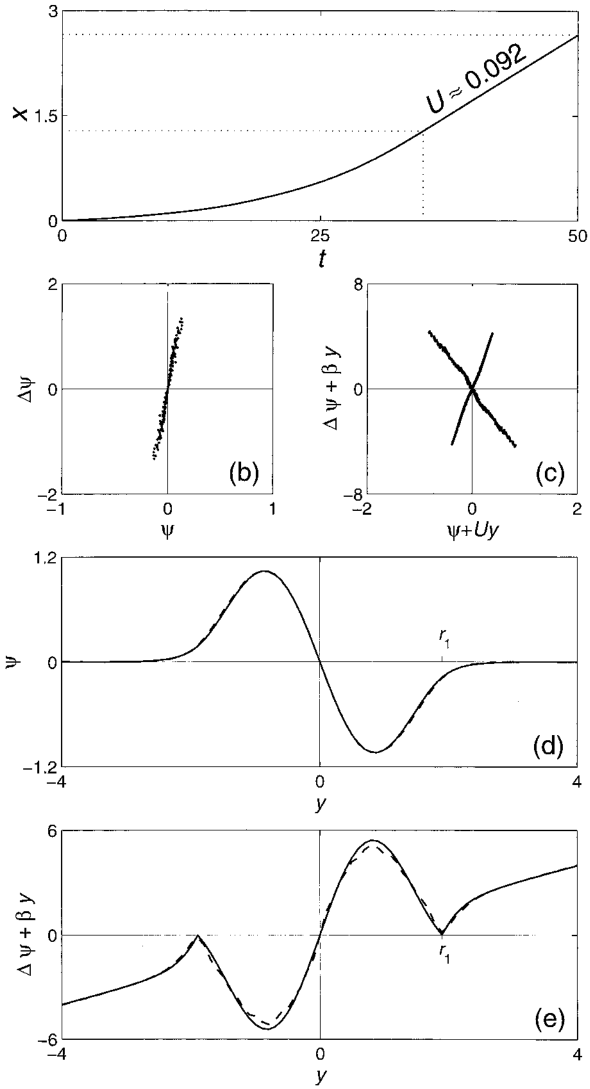

Figure 13. Identification of the dipole that developed into a Larichev and Reznik modon (Fig. 12c–f) in the course of the evolution of the perturbed Stern modon (solution (5) at $r_0 = 2.35$ and $s = 0$) at $t = 40$: the x-coordinate of max ζ vs. time (a); correlation between $\nabla^2\psi$ and ψ (b); scatter diagram of ζ vs. Ψ (c); computed solution (dashed line) and fitted exact solution (5), (6) (solid line) in terms of streamfunction (d) and potential vorticity (e).

Linearization of Eq. (3) then implies:

$$\frac{\partial}{\partial t}\omega + \frac{\partial(\psi_S, \omega)}{\partial(x, y)} + \frac{\partial(\varphi, \zeta_S)}{\partial(x, y)} = 0. \tag{10}$$

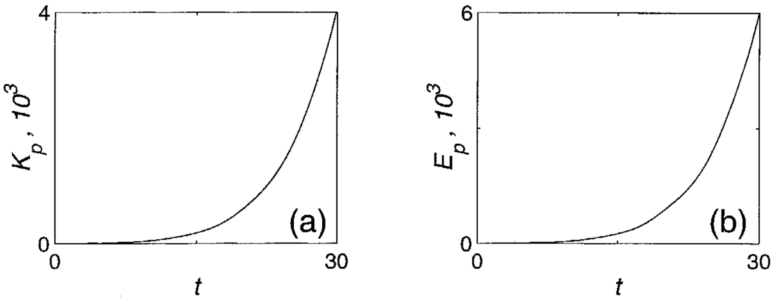

Figure 14. Exponential growth of the kinetic energy (a) and enstrophy (b) of the perturbation (K_P and E_P are normalized to their initial values).

Eqs. (9), (10) were solved numerically using the method similar to that described in Section 3. The initial perturbation was again given by (7) with φ replaced for ψ. The boundary conditions assumed were the same as for ψ: periodicity in the x-direction and $\varphi = 0$ at the northern and southern boundaries. Whereas the "mixed" (or linear with respect to the perturbation) components of the total kinetic energy and enstrophy,

$$K_{MX} = \int_{-X}^{X} dx \int_{-Y}^{Y} \left(\frac{\partial \psi_S}{\partial x} \frac{\partial \varphi}{\partial x} + \frac{\partial \psi_S}{\partial y} \frac{\partial \varphi}{\partial y} \right) dy, \qquad E_{MX} = \int_{-X}^{X} dx \int_{-Y}^{Y} \zeta_S \omega dy,$$

can be shown to be conserved (thus serving to control the computational process), the kinetic energy, K_p, and enstrophy, E_p, of the perturbation itself,

$$K_P = \frac{1}{2} \int_{-X}^{X} dx \int_{-Y}^{Y} \left[\left(\frac{\partial \varphi}{\partial x} \right)^2 + \left(\frac{\partial \varphi}{\partial y} \right)^2 \right] dy, \qquad E_P = \int_{-X}^{X} dx \int_{-Y}^{Y} \omega^2 \, dy,$$

exhibit an exponential increase in time, which is typical for linear instability (Fig. 14). It is pertinent to note that no significant growth of E_P and K_P was observed within $300T$ in a test experiment with a notoriously stable zonal flow. Although numerical simulation cannot be regarded as strict evidence (especially in such a delicate field as the linear stability analysis), this result supports the above conclusion regarding the instability (or feeble stability) of Stern's modon.

Our experiments with the Stern shielded modons (Eq. (5) at $s = 0$, $r_0 = 3.5$ and $pr_0 = j_{2,2} \approx 8.417$) proved the instability of these structures (Fig. 15), their evolution being generally similar to (though slower than) that of the Larichev and Reznik shielded modon (cf. Fig. 1).

5. Conclusion

We have cited only a few out of a great number of experiments performed with the vortex structures given by Eq. (5) and (7). In most of our simulations, collapse of unstable structures resulted in emission of vortex pairs traveling both east and west and exhibiting

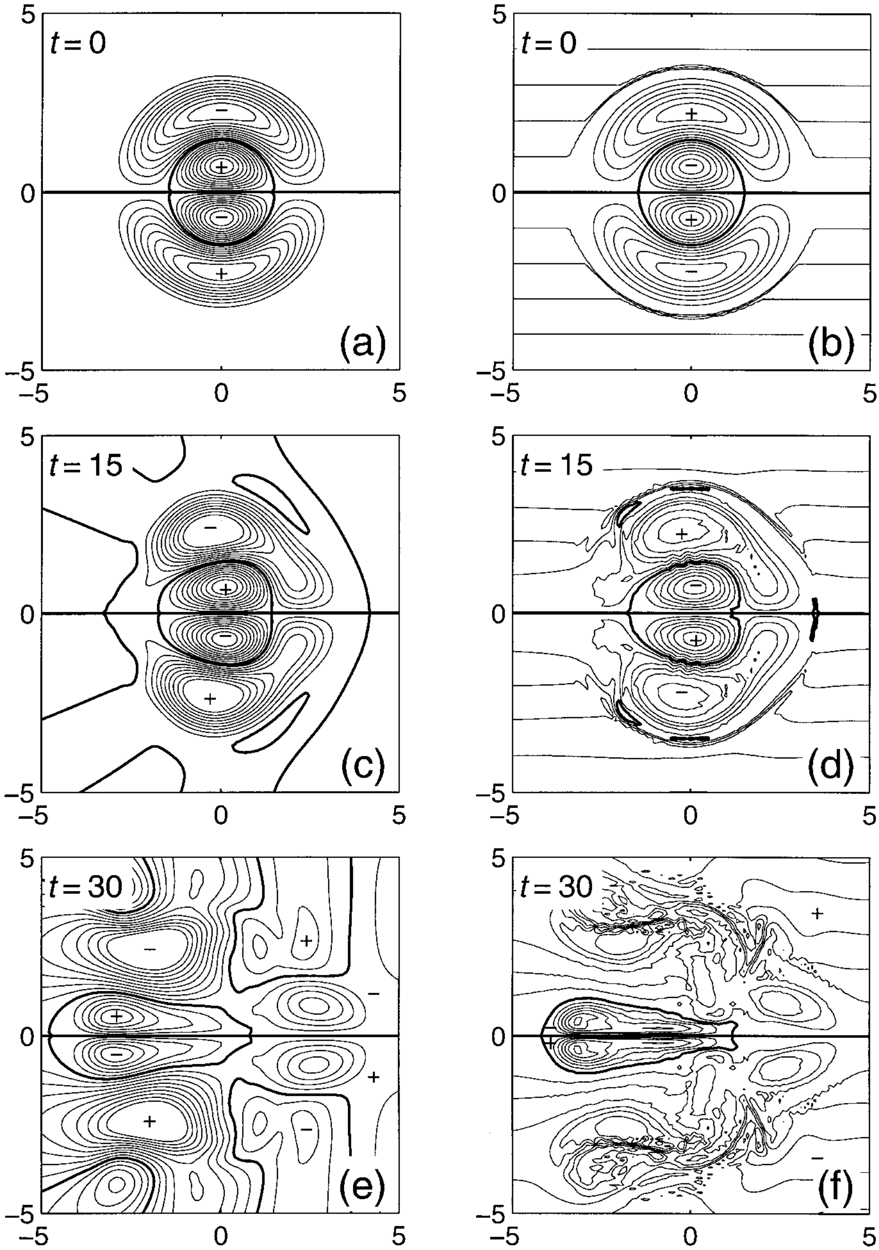

Figure 15. Collapse of the Stern shielded modon determined by Eq. (5) at $r_0 = 3.5$ and $s = 0$ in terms of streamfunction (on the left—a, c, e) and potential vorticity (on the right—b, d, f).

high survival. These paired vortices can be identified as Larichev and Reznik modons or modons of the type described by Eq. (8), respectively. Our results suggest that the emergence of long-lived modons from collapsing vortex structures might be an important factor determining the abundance of paired vortices in the ocean. They also suggest that along with the Rossby solitions propagating toward the east, the westward nonlocal modons (i.e., cores of nonlinear Rossby waves) may play a large role in forming the mesoscale pattern of the ocean currents. In all likelihood, some of the paired vortices observed in different parts of the ocean and described in the literature (see Introduction) can be associated with such westward modons.

Our experiments indicate that the Stern modon is unstable (or feebly stable) in the sense that some small perturbations cause its slow westward drift and subsequent decay, while others may lead to its slow transformation into an eastward-propagating Larichev and Reznik modon. This inference is supported by the results of a numerical integration of the linear stability problem.

Acknowledgments. We thank the referees for helpful comments. Our particular gratitude is addressed to Dr. Timour Radko, whose penetrating remarks have contributed appreciably to the improvement of the manuscript.

REFERENCES

Ahlnas, K., T. C. Royer and T. H. George. 1987. Multiple dipole eddies in Alaska Coastal Current detected with Landsat Thematic Mapper data. J. Geophys. Res., *92,* 13041–13047.

Berestov, A. L. 1979. Solitary Rossby waves. Izv. Acad. Sci., USSR., Atmos. Oceanic Phys., *15,* 648–654.

—— 1981. Some new solutions for the Rossby solitions. Izv. Acad. Sci., USSR., Atmos. Oceanic Phys., *17,* 82–87.

Boyd, J. P. 1994. Nonlocal modons on the beta-plane. Geophys. Astrophys. Fluid Dyn. *75,* 163–182.

Boyd, J. P. and H. Ma. 1990. Numerical study of elliptical modons using a spectral method. J. Fluid Mech., *221,* 597–611.

Flierl, G. R. 1987. Isolated eddy models in geophysics. Ann. Rev. Fluid Mech., *19,* 493–530.

Flierl, G. R. and K. Haines. 1994. The decay of modons due to Rossby wave radiation. Phys. Fluids, *6A,* 3487–3497.

Flierl, G. R., V. D. Larichev, J. C. McWilliams and G. M. Reznik. 1980. The dynamics of baroclinic and barotropic solitary eddies. Dyn. Atmos. Oceans, *5,* 1–41.

Haupt, S. E., J. C. McWilliams and J. J. Tribbia. 1993. Modons in shear-flow. J. Atmos. Sci., *50,* 1181–1198.

Hesthaven, J. P. Lynov, A. H. Nielsen, J. J. Rassmussen, M. R. Schmidt, E. G. Shapiro and S. K. Turitsyn. 1995. Dynamics of a nonlinear dipole vortex. Phys. Fluids *7,* 2220–2229.

Hesthaven, J. S., J. P. Lynov and J. Nycander. 1993. Dynamics of nonstationary dipole vortices. Phys. Fluids, *5A,* 622–629.

Hooker, S. B., J. W. Brown and A. D. Kirwan Jr. 1995a. Detecting ‘‘dipole ring’’ separatrices with zebra palettes. IEEE Trans. Geosci. Remote Sens. *33,* 1306–1312.

Hooker, S. B. Brown, J. W., Kirwan, A. D. Jr., Lindemann, G. J. and R. P. Mied. 1995b. Kinematics of a warm-core dipole ring. J. Geophys. Res., *100* (C12), 24797–24809.

Ikeda, M. and W. J. Emery. 1984. Satellite observations and modelling of meanders in the California Current system off Oregon and Northern California, J. Phys. Oceanogr., *14,* 1434–1450.

Ikeda, M., L. A. Mysak and W. J. Emery. 1984. Observation and modelling of satellite-sensed meanders and eddies off Vancouver Island. J. Phys. Oceanogr., *14,* 3–20.

Johannessen, J. A., Svendsen, E., Sandven, S., Johannessen, O. M. and K. Legree. 1989. Three-dimensional of mesoscale eddies in the Norwegian Coastal Current. J. Phys. Oceanogr., *19,* 3–19.

Kamenkovich, V. M., M. N. Koshlyakov and A. S. Monin. 1986. Synoptic Eddies in the Ocean. Reidel, The Netherlands, 475 pp.

Kennelly, M. A., Evans, R. H. and T. M. Joyce. 1985. Small-scale cyclones on the periphery of a Gulf-Stream warm-core ring. J. Geophys. Res., *90,* 8845–8857.

Kizner, Z. I. 1984. Rossby solitons with axisymmetric baroclinic modes. Rep. Doklady USSR. Acad. Sci., *275,* 1495–1498.

—— 1988. On the theory of intrathermocline eddies. Rep. Doklady USSR. Acad. Sci., *300,* 453–457.

—— 1997. Solitary Rossby waves with baroclinic modes. J. Mar. Res., *55,* 671–685.

Lamb, H. 1932. Hydrodynamics, 6th ed. Dover, New York, NY, 738 pp.

Larichev, V. D. 1983a. General features of nonlinear synoptic dynamics in the simple model of a barotropic ocean. Oceanologia, *23,* 551–558.

—— 1983b. Qualitative analysis of nonlinear evolution of localized perturbations on a β-plane. Oceanologia, *23,* 1303–1311.

Larichev, V. D. and G. M. Reznik. 1976. Two-dimensional solitary Rossby waves. Rep. Doklady USSR. Acad. Sci., *231,* 1077–1080.

—— 1982. Numerical experiments on the study of collision of two-dimensional solitary Rossby waves. Rep. Doklady USSR. Acad. Sci., *264,* 229–233.

—— 1983. Colliding two-dimensional solitary Rossby waves. Oceanologia, *23,* 725–734.

Makino, M., T. Kamimura and T. Taniuti. 1981. Dynamics of two-dimensional solitary vortices in a low-β plasma with convective motion. J. Phys. Soc. Japan, *50,* 980–989.

McWilliams, J. J. 1983. Interactions of isolated vortices. II Modon generation by monopole collision. Geophys. Astrophys. Fluid Dyn., *24,* 1–24.

McWilliams, J. J. and G. R. Flierl. 1979. On the evolution of isolated, nonlinear vortices. J. Phys. Oceanogr., *9,* 1155–1182.

McWilliams, J. C., G. R. Flierl, V. D. Larichev and G. M. Reznik. 1981. Numerical studies of barotropic modons. Dyn. Atmos. Oceans, *5,* 219–238.

McWilliams, J. C. and N. J. Zabusky. 1982. Interactions of isolated vortices. I: Modons colliding with modons. Geophys. Astrophys. Fluid Dyn., *19,* 207–227.

Mezinger, F. and A. Arakawa. 1976. Numerical models used in atmospheric models. GARP Publication Series, 17.

Mied, R. P. and G. J. Lindemann. 1982. The birth and evolution of eastward-propagating modons. J. Phys. Oceanogr., *12,* 213–230.

Nogan, K., S. Meacham and P. J. Morrison. 1996. Elliptical vortices in shear: Hamiltonian moment formulation and Melnikov analysis. Phys. Fluids, *8,* 896–913.

Nycander, J. 1988. New stationary vortex solutions of the Hasegawa-Mima equation. J. Plasma Phys., *39,* 418–428.

—— 1992. Refutation of stability proofs for dipole vertices. Phys. Fluids, *4A,* 467–476.

—— 1994. Steady vortices in plasmas and geophysical flows. Chaos, *4,* 253–267.

Orlandi, P., R. Verzicco and G. J. F. van Heijst. 1994. Stability of shielded vortex dipoles, *in* Modelling of Oceanic Vortices, G. J. F. van Heijst, ed., North Holland, Amsterdam, 169–176.

Samarsky, A. A. 1989. Theory of finite-difference schemes. Moscow, Nauka, 616 pp.

Stern, M. E. 1975. Minimal properties of planetary eddies. J. Mar. Res., *33,* 1–13.

Thomson, R. E. 1984. A cyclonic eddy over the continental margin of Vancouver Island: Evidence for baroclinic instability. J. Phys. Oceanogr., *14,* 1326–1348.

Tribbia, J. J. 1984. Modons in spherical geometry. Geophys. Astrophys. Fluid Dyn. *30,* 131–168.

Verkley, W. T. M. 1984. The construction of barotropic modons on a sphere. J. Atmos. Sci., *41,* 2492–2504.

Received: *17 November, 1998;* revised: *27 March, 2000.*